Int. J. Nonlinear Anal. Appl. 14 (2023) 11, 241–249
ISSN: 2008-6822 (electronic)
http://dx.doi.org/10.22075/ijnaa.2023.29848.4276

Application of graph theory and canonical forms in reliability analysis of symmetric structures

Ali Asghar Bagheri[a], Alireza Mortezaei[a,b,*], Mohammad Ali Sayarinejad[c]

[a] Department of Civil Engineering, Semnan Branch, Islamic Azad University, Semnan, Iran

[b] Seismic Geotechnical and High Performance Concrete Research Centre

[c] Department of Civil Engineering, Qaemshahr Branch, Islamic Azad University, Qaemshahr, Iran

(Communicated by Asadollah Aghajani)

Abstract

Many abilities of Monte Carlo simulation methods have led to their increasing use in solving various reliability problems of structures. These methods are based on generating random samples in order to simulate events and estimate their results. Achieving certain accuracy requires a significant number of simulation operations. Acceptable accuracies can be achieved with a smaller number of samples by adopting different approaches. In this article, for the first time, symmetric structures are analyzed using the theory of graphs and canonical forms, the frequency of the structures is calculated, and their reliability is also checked using these theories. Also, the study and investigation of the calculation of frequencies and eigenvectors corresponding to symmetric structural models from the point of view of the decomposition of the stiffness matrix in probabilistic reliability analysis, which we will achieve this goal by using the proposed theories. In this article, in addition to obtaining all canonical forms, the relationship between all canonical forms is obtained. Finally, a new Rayleigh-based theory called the proposed improved Rayleigh theory is presented, which is used to extract the natural frequencies of structures. Also, in this research, several samples of different frames and structures were presented using the proposed method and finally, numerical results were presented and the solution of the three-story frame with 24 degrees of freedom was presented. It can be seen from the results that the proposed method has a much higher speed and accuracy than the Monte Carlo method.

Keywords: canonical forms, improved Rayleigh-Ritz method, graph, symmetrical structure analysis
2020 MSC: 37M05

1 Introduction

Engineering structures are subjected to environmental loads that are inherently random in nature [19]. On the other hand, mechanical parameters of structural materials such as material properties and geometrical conditions of the structure in terms of dimensions and boundary conditions in general are basic sources uncertainty in a structure are considered [14]. The random nature of the loads and mechanical parameters of the materials and geometry of the structure can result in the random performance of the structure at the operational level. Therefore, evaluating

*Corresponding author
Email addresses: Bagheri.110sari2016@yahoo.com (Ali Asghar Bagheri), a.mortezaei@semnaniau.ac.ir (Alireza Mortezaei), m.sayarinejad@qaemiau.ac.ir (Mohammad Ali Sayarinejad)

Received: November 2022 *Accepted:* February 2023

and estimating the probability of failure at the level of the structure's operation, taking into account the types of uncertainty, is of particular importance in estimating the level of safety of the structure [15]. Useful probabilistic methods of reliability of structures can be used to estimate the safety of the structure (estimate the probability of failure). The methods of estimating the probability of failure of a structure are mainly divided into two categories, analytical methods and simulation methods [18].

Appropriate estimation is important to estimate the probability of failure in the reliability analysis of structures. For this purpose, methods such as: Hasofer-Lind method, stable transfer method, simulation methods such as Monte Carlo, fuzzy index of structures and methods based on gradient vector have been widely used by structural engineers and many articles try to have developed or optimized existing methods. The existence of symmetry reduces the dimensions of the problem and the dimensions of the corresponding matrices, and therefore, it reduces the problem necessary to implement numerical algorithms in computers and increases the speed of its execution, and it is clear that it controls the propagation of calculation errors. This importance appears when we will face large-scale structures. One of the goals of this article is to study and investigate the calculation of frequencies and eigenvectors corresponding to symmetric structural models from the perspective of stiffness matrix decomposition in a probabilistic reliability analysis.

2 Monte Carlo simulation method

This method has many applications in the analysis of discrete random processes as well as complex reliability problems with a limit condition function containing several maximum possible points. Monte Carlo method can be used to estimate the probability of failure based on three basic steps as follows:

1. Random generation of numbers using the cumulative probability distribution function of random variables in the range of zero and one $X \in [0, 1]$
2. Estimating the value of each random variable using the statistical properties of random variables based on the randomly generated number in step one
3. Estimation of the limit condition function according to the data generated in the second step and estimation of the failure probability

Monte Carlo simulation method is a simple random sampling method based on creating a sequence of random samples where each random variable X_i is randomly sampled and then the limit state function is checked. If $g(X_i) \leq 0$ is established, in such a case, the generated sample of random data X_i is placed in the failure area and otherwise in the health area. This test (simulator of random variables with limit state function control) requires a large number of repetitions, in each of these times the vector X_i is randomly selected to produce several points in the failure zone.

3 Literature review

In Kaveh and Sayarinejad's paper, the first-order reliability- based method (FORM) is presented for reliability sensitivity calculation of a structural system with linear limit state function and normal random variables. They also used Monte Carlo simulation to estimate reliability sensitivity and proposed a method to use first order deviation for sensitivity analysis of random variables. In most of these methods, it is assumed that random variables have cognitive uncertainty, which means that all parameters of random variables are certain. However, in engineering problems, all random variables are unrealistic because there is both cognitive uncertainty and stochastic uncertainty in the random variable. Random uncertainty is the result of insufficient information, under-sampling data or missing data. While cognitive uncertainty is the essence of variables [8, 9, 11].

Researchers conducted many studies on sensitivity analysis based on P-BOX [3, 12]. Nevertheless, sensitivity analysis is suggested to be slightly different from reliability sensitivity analysis. Also, methods based on Monte Carlo simulation (MCS) have been widely used in reliability sensitivity analysis. For example, [10] proposed a Monte Carlo simulation-based sensitivity estimation method [5]. They provided an efficient method to estimate Monte Carlo simulation-based sensitivity parameters. Therefore, these methods are only based on stochastic uncertainty instead of using both cognitive uncertainty and stochastic uncertainty. In this work, by putting together P-BOX principle, interval algorithm, FORM method, Monte Carlo simulation and using the methods of papers [5, 9], a single reliability sensitivity estimation method including both a accidently uncertainty and cognitive uncertainty was suggested.

In 2018, Burukhina and colleagues formed a reliability matrix based on a distinct matrix of special matrices and continuity matrices for the analysis of structural designs, where the probability of failure and success of the system is equal to the reliability matrix, which can be used to reduce time and the volume of structural software calculations used [2]. In 1988, Johnson investigated the effect of variables such as materials, equipment, human factors and the environment in the calculation of structural stress and strength [6]. In 2013, Fragiadakis and Christodoulou proposed a simple and small-scale network based on the real scale by using graph theory and calculating reliability with Monte Carlo simulation to get an estimate of the probability of failure at the desired level [4]. In 2013, using several samples that were subjected to seismic stimulation and under the control of active systems, Shariatmadar and Behnam Rad showed the evaluation method by simulating a subset in the probability of rupture of areas with complex rupture and a large number of random variables is an efficient method and powerful [17]. In 2017, Lehký, et al. discussed the advantages and disadvantages of these two methods with two techniques of simulating small samples of artificial neural networks and using inverse reliability in the design of reinforced concrete beams and slabs, etc. [13]. In 2017, Nabian and Meidani studied and predicted basic systems from the classified replacement of determined connection networks and the end-to-end replacement of a number of components specified and determined connections as well as the average connections for the study based on the simulation of two terminals of the California transportation network connections based on the maximum probability of an earthquake through an in-depth study of neural networks to accelerate the reliability analysis [16]. In 2012, Bhattacharyya and Johnson were able to obtain more reliable and accurate results for the calculation of stress and resistance in reliability systems by studying limited samples to Monte Carlo simulation with asymptotic distribution of developed samples [1].

4 Concepts of graph theory

A graph $G(N;M)$ consists of a set of nodes (vertices) and a set of member elements (edges) with an incidence relation that associates a pair of nodes with each member. Two nodes are adjacent if they match the same member. A graph G is called undirected if a member of a pair of nodes is unordered.

In linear algebra, two matrices A and B are called similar if:

$$B = P^{-1}AP \tag{4.1}$$

where P is a non-singular matrix and the transformation $A \to B$ is known as the similarity transformation of A. The characteristic polynomial of a square matrix A is a polynomial of the form $P(\lambda) = \det(A - \lambda I)$, which is stable under matrix similarity and has eigenvalues as roots. A scalar number λ is an eigenvalue of A if there exists a nonzero vector v, known as an eigenvector, such that:

$$Av = \lambda v \tag{4.2}$$

$$(\lambda I - A)v = 0. \tag{4.3}$$

The characteristic polynomial of a diagonal matrix A is easily defined. If the diagonal entries of A are $a_1.a_2; a_3; ...; a_n$, then:

$$(a_1 - \lambda)(a_2 - \lambda)(a_3 - \lambda)...(a_n - \lambda) = 0 \tag{4.4}$$

A will be the characteristic polynomial. According to Eq. (4.4), it can be seen that the diagonal entries are also eigenvalues of this matrix. The simplest matrix to find the eigenvalues of is a diagonal matrix. Similarly, the eigenvalues of a triangular matrix are its diagonal entries.

A matrix can have imaginary eigenvalues because its characteristic polynomial can have real or mixed roots. Every $n \times n$ matrix has exactly n imaginary and real eigenvalues, which are counted by multiplicity.

The adjacency matrix A of the graph G whose nodes are labeled n is defined as follows:

$$a_{ij} = \begin{cases} 1, & \text{if node } n_i \text{ is adjacent to } n_i; \\ 0, & \text{otherwise.} \end{cases} \tag{4.5}$$

The degree matrix $D = [dij]nn$ is a diagonal matrix containing the degree of node, where dii is the degree of node i. The Laplacian matrix $L = [lij]nn$ is defined as follows:

$$L = D - A. \tag{4.6}$$

Therefore, the inputs of region L are:

$$a_{ij} = \begin{cases} -1, & \text{if node } n_i \text{ is adjacent to } n_i; \\ deg(n_i), & \text{if } i = j; \\ 0, & \text{otherwise} \end{cases} \tag{4.7}$$

To solve the special adjacency matrix, consider the special problem as follows:

$$Av_i = \lambda_i v_i \tag{4.8}$$

where λ_i is the i^{th} eigenvalue and v_i is the corresponding eigenvector. For A to be a real symmetric matrix, all the corresponding eigenvalues in the form of equation (4.9) are real:

$$\lambda_1 \leq \lambda_2 \leq \lambda_3 \leq ... \leq \lambda_{n-1} \leq \lambda_n \tag{4.9}$$

The largest eigenvalue λ_n has a multiplicity equal to unity for the characteristic equation A. The corresponding eigenvector v_n is the only eigenvector with positive entries. This vector has many interesting properties that are used in structural mechanics. For the special solution of the Laplacian matrix, consider the problem as follows:

$$L_{v_i} = \lambda_i v_i \tag{4.10}$$

where λ_i is the i^{th} eigenvalue and v_i is the corresponding eigenvector. Since A is a real symmetric matrix and all its eigenvalues are real, all eigenvalues of L are also real. It can be shown that the matrix L is a positive semi-definite matrix by:

$$0 = \lambda_1 \leq \lambda_2 \leq \lambda_3 \leq ... \leq \lambda_{n-1} \leq \lambda_n \tag{4.11}$$

$$v_1 = \{1.1.1...1\}. \tag{4.12}$$

The second eigenvalue λ_2 of L is also known as the "algebraic connection" of the graph, and its eigenvector v_2 is called the Fiedler vector. This vector has interesting properties. Kronecker product of two matrices is an operation on these matrices that results in a block matrix. This operation is denoted by $\bigotimes$. Kronecker product of two matrices A_{mn} and B_{pq} is the block matrix $mp \times nq$ in the form:

$$A_{m\times n} \bigotimes B_{p\times q} = \begin{bmatrix} a_{11}B & \cdots & a_{1n}B \\ \vdots & \ddots & \vdots \\ a_{m1}B & \cdots & a_{1n}B \end{bmatrix}_{mp\times nq} \tag{4.13}$$

A Hermitian matrix is a square matrix equal to its conjugate transpose. A real matrix is Hermitian if and only if it is symmetric. Being Hermitian is a necessary condition for a matrix to be diagonal:

$$\text{A is Hermitian} \iff a_{ij} = \overline{a_{ji}}. \tag{4.14}$$

For two matrices A_1 and A_2 to be diagonalizable simultaneously, these two matrices must be Hermitian and the substitution $A_1 A_2 = A_2 A_1$.

5 Canonical forms of a matrix

In this section, all existing canonical forms for structures with two-way symmetry and rotational repeating structures are presented. Here, M is a matrix whose elements consist entirely of real numbers. Canonical forms I, II, III and IV were presented by Kala [7, 8].

5.1 Canonical form I

In this figure, M is a diagonal block matrix whose pattern is shown in Eq. (5.1):

$$M_{2n} = \begin{bmatrix} A_n & 0 \\ 0 & A_n \end{bmatrix}_{2n\times 2n} \tag{5.1}$$

Since M is a diagonal matrix, its determinant can be calculated as follows:

$$\det(M) = \det(A) \times \det(A) \tag{5.2}$$

Moreover, the set of eigenvalues of submatrix A is equal to λA. Therefore, the eigenvalues of M can be calculated as Eq. (5.3).

$$\lambda_M = \{\lambda_A\} \cup \{\lambda_A\} \tag{5.3}$$

This form can be generalized by placing a large number of matrices of different dimensions on its main diagonal entries. According to Eq. (5.3), the eigenvalues of this generalized matrix will be equal to the union of the eigenvalues of those matrices located in its main diameter.

5.2 Canonical form II

As shown in Eq. (5.4), for this particular form, the matrix M has a pattern:

$$M_{2n} = \begin{bmatrix} A_n & B_n \\ B_n & A_n \end{bmatrix}_{2n\times 2n} \tag{5.4}$$

By adding the second column to the first column and then subtracting the first row from the second column, M becomes an upper triangular matrix as follows:

$$M_{2n} = \begin{bmatrix} A_n & B_n \\ B_n & A_n \end{bmatrix} = \begin{bmatrix} C_n & B_n \\ 0 & D_n \end{bmatrix} \tag{5.5}$$

where

$$C = [A] + [B] \tag{5.6}$$

$$D = [A] - [B] \tag{5.7}$$

Since M is a triangular matrix, its determinant is equal to the product of two matrices lying on the diameter of M. Therefore, the set of eigenvalues of M can be obtained as Eq. (5.8):

$$\lambda_M = \{\lambda_C\} \cup \{\lambda_D\} \tag{5.8}$$

5.3 Canonical form III

In this figure, M has an $N \times N$ submatrix where $N = 2n$. Form II pattern is reinforced with k rows and k columns as formulated in Eq. (23):

$$M = \begin{bmatrix} A & B & P \\ B & A & P \\ Q & H & R \end{bmatrix} \tag{5.9}$$

As can be seen, M is an $(N + k) \times (N + k)$ matrix and the entries of the augmented columns are the same in each column. Similar to form II, in this case, M can be factored using row and column permutation. By replacing the second column and the second row with the fourth column and the fourth row respectively, the fourth column is added to the first column. In the last step, by reducing the first row from the fourth row, M becomes an upper triangular matrix in the form of Eq. (5.10):

$$M = \begin{bmatrix} A+B & P & B \\ Q+H & R & H \\ 0 & 0 & A-B \end{bmatrix} = \begin{bmatrix} E & K \\ 0 & D \end{bmatrix} \tag{5.10}$$

where

$$E = \begin{bmatrix} A+B & P \\ Q+H & R \end{bmatrix} \tag{5.11}$$

$$D = [A] - [B] \tag{5.12}$$

Since M is a triangular matrix, its determinant is equal to the product of two matrices that lie on the diagonal entries. Therefore, the set of eigenvalues of M can be obtained as Eq. (5.13):

$$\lambda_M = \{\lambda_E\} \cup \{\lambda_D\} \tag{5.13}$$

5.4 Canonical form IV

M is a $6n \times 6n$ matrix with the following pattern:

$$M = \begin{bmatrix} S-H & H-S & & & & \\ H-S & S & -H & & & \\ & -H & S & H-S & & \\ & & H-S & S & -H & \\ & & & -H & S & H-S \\ & & & & H-S & S-H \end{bmatrix} \tag{5.14}$$

S and H are $n \times n$ matrices. The characteristic polynomial of M can be calculated through Eq. (5.15):

$$P_M(\lambda) = [\lambda(2H - 2S + \lambda)][\lambda^2 - 2S\lambda + SH - H^2][\lambda^2 - 2S\lambda + 3SH + -3H^2] \tag{5.15}$$

The first term of the Eq. (5.15) can be considered as the characteristic polynomial of the matrix, which is a matrix of the form II of Eq. (5.16):

$$[E_1] = \begin{bmatrix} S-H & H-S \\ H-S & S-H \end{bmatrix} = \lambda_{(2S-2H)} \cup \lambda_{[0]_{n\times n}} \tag{5.16}$$

The second term of Eq. (5.15) can be considered as the characteristic polynomial of the matrix in Eq. (5.17):

$$[E_2] = \begin{bmatrix} S+H & -S \\ H-S & S-H \end{bmatrix} \tag{5.17}$$

The third term of Eq. (5.15) can be considered as the characteristic polynomial of the matrix in Eq. (5.18):

$$[E_2] = \begin{bmatrix} S+H & -S \\ H-S & S-H \end{bmatrix} \tag{5.18}$$

Hence, to find the eigenvalues of a matrix in the form of Eq. (5.14), calculate the eigenvalues E_i for $i = 1.2$ and 3 are enough:

$$\lambda_M = \{\lambda_{E_1}\} \cup \{\lambda_{E_2}\} \cup \{\lambda_{E_3}\} \tag{5.19}$$

6 The model of the investigated structure

If we consider a three-story bending frame with 24 degrees of translational freedom, we want to use the minimum and maximum frequencies created in this frame to evaluate the reliability of the nodes in the face of failure or failure. We know that the vibration period T actually expresses the physical and behavioral characteristics of the system in contrast to dynamic movement, and because it has an inverse relationship with stiffness, it is another expression of stiffness. Also, the determination of the vibration period of the system, T_n of the structure is dependent on the determination of the frequency ω_n, because:

$$T_n = \frac{2\pi}{\omega_n} = 2\pi\sqrt{\frac{m}{k}}. \tag{6.1}$$

Considering that the determination of vibration characteristics including frequencies and natural modes of a structure requires solving the matrix of the eigenvalue problem and other similar methods, first of all, the methods of determining the natural vibration period of the structure should be addressed using analytical, experimental and software relationships. Then, the concepts of reliability assessment of structures and Monte Carlo simulation will be examined, and finally, by introducing the graph method and canonical standard forms, a new method will be mentioned in the process of calculating the reliability of structures.

7 Investigating the solution of the three-story frame with 24 degrees of freedom

In current paper, a three-story frame with 24 degrees of freedom has been considered as a model order to check the detailed method solution. It should be noted that to apply the boundary conditions of the free edge and the cantilever edge, we consider the stiffness of the hypothetical springs at the edges of the three-story frame to be equal to 0 and 10^{20}, respectively. Also, we consider the abbreviations of F and C for the boundary conditions for the free edge and for the cantilever edge, respectively.

According to the results presented in the given tables (1,2), it can be seen that the correctness of the rapid convergence of the exact solutions provided in the proposed method and Monte Carlo is quite evident, and from the results obtained, it can be concluded that in the proposed method and Monte Carlo Found in the value of the improved Fourier series expansion index of 14×14, we can achieve acceptable results.

Now, in the following, we analyze the effects of changes in the geometric parameters of the three-story frame on the in-plane free vibrations of the three-story frame using the detailed solution provided.

Table 1: Natural frequency of three-story frame (HZ) with dimensions $\frac{a}{b}=1$ with FFFF boundary conditions

method	$M\times N$	Mod number							
		1	2	3	4	5	6	7	8
Improved Rayleigh-Ritz Method	6×6	1423.257	1545.124	1545.124	1634.903	2243.338	2704.183	2643.552	2643.552
	8×8	1322.661	1411.426	1411.426	1494.359	1702.13	1961.774	2123.657	2123.657
	10×10	1314.07	1400.556	1400.556	1486.652	1690.889	1953.328	2110.096	2110.096
	12×12	1313.244	1399.647	1399.647	1486.266	1690.35	1953.27	2109.611	2109.611
	14×14	1313.152	1399.312	1399.312	1486.147	1689.927	1953.211	2109.443	2109.443
ANSYS		1311.5	1397.3	1397.3	1484.9	1687.7	1950.5	2105.8	2105.8

Table 2: Natural frequency of three-story frame (HZ) with dimensions $\frac{a}{b}=1$ with CCCC boundary conditions

method	$M\times N$	Mod number							
		1	2	3	4	5	6	7	8
improved Rayleigh-Ritz method	6×6	2301.44	2301.44	2503.494	3287.837	5137.24	4661.084	4661.084	5907.18
	8×8	2022.064	2022.064	2402.481	2956.612	3351.242	3372.441	3372.441	3835.35
	10×10	2013.728	2013.728	2398.841	2939.247	3322.406	3348.41	3348.41	3802.664
	12×12	2012.207	2012.207	2397.432	2937.006	3319.004	3345.741	3345.741	3798.842
	14×14	2011.806	2011.806	2397.384	2936.575	3318.805	3344.405	3344.405	3798.577
ANSYS		2008.6	2008.6	2395.2	2932.9	3316	3340.4	3340.4	3795.4

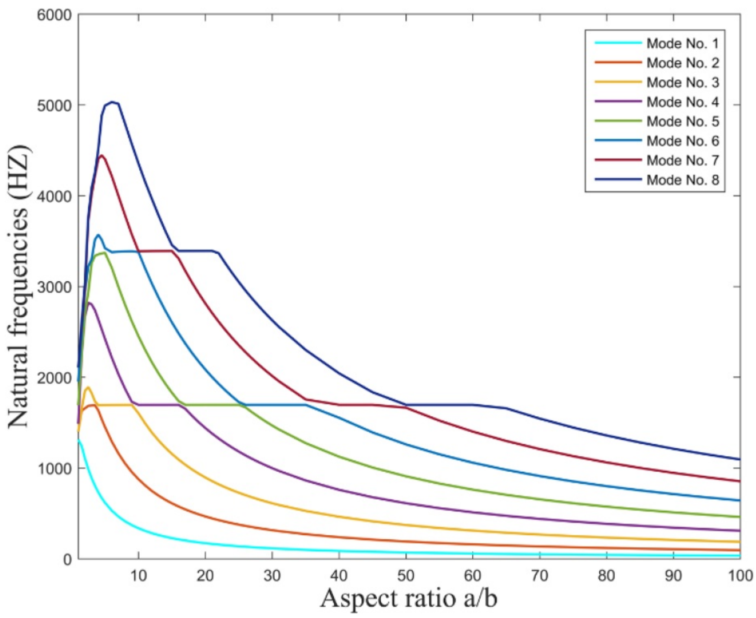

Figure 1: Investigating the effects of changes in the aspect ratio on the natural frequencies of the three-story frame extracted from the proposed method and found by Monte Carlo for CCCC boundary conditions.

In Fig. 1, it can be seen that the natural frequencies for the first mode shape decrease with the increase of the aspect ratio $\frac{a}{b}$ from the beginning, but the natural frequencies for the second to eighth mode shape increase up to a value of the aspect ratio and Then, after that, the aspect ratio value starts to decrease. And this downward trend continues until after the value of the aspect ratio $\frac{a}{b}=100$ natural frequencies remain almost constant.

In Fig. 2, it can be seen that the natural frequencies for the first mode shape increase linearly with the increase of the aspect ratio $\frac{a}{b}$ from the very beginning, but the natural frequencies for the second to eighth modes shape up to a value of the aspect ratio. First, it increases non-linearly, and this non-linear upward trend continues until the natural frequencies increase linearly after a certain value of the $\frac{a}{b}$ aspect ratio.

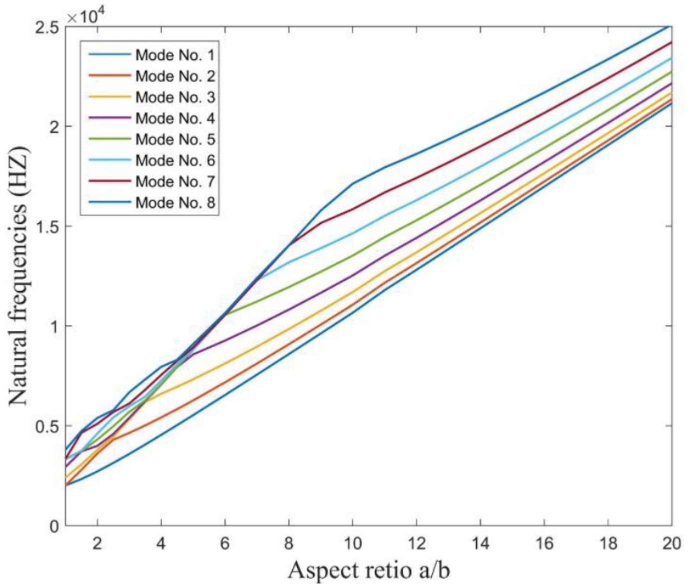

Figure 2: Investigating the effects of changes in the aspect ratio on the natural frequencies of the three-story frame extracted from the proposed method and found by Monte Carlo for CCCC boundary conditions.

In Fig. 3, it can be seen that the natural frequencies for the first to third mode shape decrease with the increase of the aspect ratio $\frac{a}{b}$ from the very beginning, but the natural frequencies for the fourth to eighth mode shape increase up to a value of the aspect ratio. And then after that, the aspect ratio value starts to decrease. And this downward trend continues until the natural frequencies remain almost constant after the value of the aspect ratio $\frac{a}{b} = 150$, which if we compare these results with the results of the three-story frame with CCCC boundary conditions We can see that the natural frequency values in the three-story frame with CFFF boundary conditions reach a constant value later.

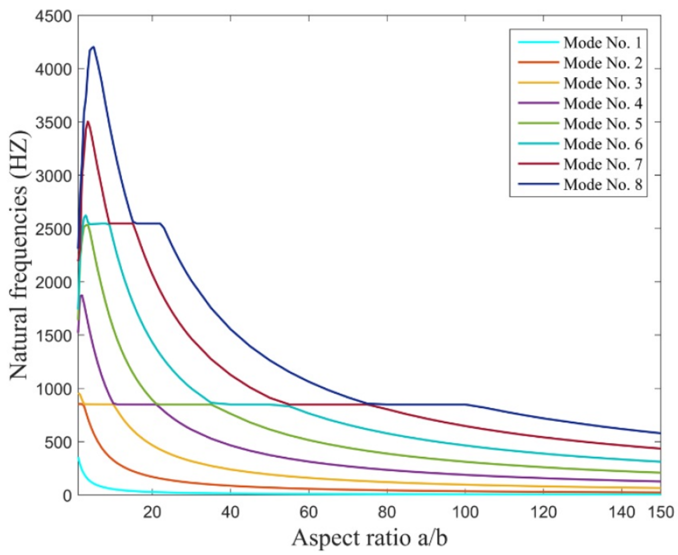

Figure 3: Investigating the effects of changes in the aspect ratio on the natural frequencies of the three-story frame extracted from the proposed method and found by Monte Carlo for CFFF boundary conditions.

8 Conclusion

In this paper, the free vibrations of a three-story frame with 24 degrees of freedom with different boundary conditions and geometrical conditions were investigated and the following results were obtained:

By using the proposed method as well as Monte Carlo simulation and the artificial spring boundary technique, all classical boundary conditions can be easily applied to the problem.

By using the displacement components of the improved Fourier series expansion in the Rayleigh-Ritz method, an accurate solution can be provided in the field of in-plane free vibrations of the three-story frame. Also, by using the improved Rayleigh-Ritz method, we will be able to investigate several issues in the field of vibrations.

By increasing the expansion indices of the improved Fourier series expansion m and n of the presented method up to the value of m=n=14, the natural frequencies of the in-plane free vibrations of the three-story frame can be extracted with good accuracy.

The natural frequencies of the free vibrations of the three-story frame decrease with the increase of the a/b aspect ratio for FFFF and CFFF boundary conditions and increase for CCCC boundary conditions.

References

[1] G.K. Bhattacharyya and R.A. Johnson, *Estimation of reliability in a multicomponent stress-strength model*, J. Amer. Statist. Assoc. *69* (2012), no. 348, 966–970.

[2] O. Burukhina, A. Bushinskaya, I. Maltceva and S. Timashev, *Mechanical system reliability analysis using reliability matrix method*, IOP Conf. Ser.: Mater. Sci. Eng. IOP Pub. **365** (2018), no. 4, 042067.

[3] Y. Chen and J. Feng, *Group-theoretic exploitations of symmetry in novel prestressed structures*, Symmetry **10** (2018), no. 6, 229.

[4] M. Fragiadakis and S.E. Christodoulou, *Seismic reliability assessment of urban water networks*, Earthquake Engin. Struct. Dyn. **43** (2013), no. 3, 357–374.

[5] O. Goldschmidt, P. Jaillet and R. Lasota, *On reliability of graphs with node failures*, Networks **24** (1994), no. 4, 251–259.

[6] R.A. Johnson, *3 Stress-Strength Models for Reliability*, Handbook of Statistics, 1988.

[7] Z. Kala, *Reliability analysis of the lateral torsional buckling resistance and the ultimate limit state of steel beams with random imperfections*, J. Civil Eng. Manag. **21** (2015), no. 7, 902–911.

[8] A. Kaveh and M.A. Sayarinezhad, *Eigenvalues of matrices with special patterns using symmetry of graph*, Sci. Iran. **10** (2003), no. 2, 220–226.

[9] A. Kaveh and M.A. Sayarinejad, *Eigensolutions for matrices of special structures*, Commun. Numer. Meth. Engin. **19** (2003), no. 2, 125–136.

[10] A. Kaveh and M.A. Sayarinejad, *Graph symmetry and dynamic systems*, Comput. Struct. **82** (2004), no. 23-26, 2229–2240.

[11] A. Kaveh and M.A. Sayarinezhad, *Eigensolution of special compound matrices and applications*, Asian J. Civil Eng. (Building and Housing) **6** (2005), no. 6, 495–509.

[12] A. Kaveh and M.A. Sayarinejad, *Eigensolution of specially structured matrices with hyper-symmetry*, Int. J. Numer. Meth. Eng. **67** (2006), no. 7, 1012–1043.

[13] D. Lehký, O. Slowik and D. Novák, *Reliability-based design: Artificial neural networks and double-loop reliability-based optimization approaches*, Adv. Eng. Software **117** (2018), 123–135.

[14] J. Li and J. Chen, *Probability density evolution method for dynamic response analysis of structures with uncertain parameters*, Comput. Mech. **34** (2004), no. 5, 400–409.

[15] J. Li and J. Chen, *Stochastic Dynamics of Structures*, John Wiley & Sons, 2009.

[16] M.A. Nabian and H. Meidani, *Deep learning for accelerated seismic reliability analysis of transportation networks*, Comput. Aided Civil Infrastruct. Engin. **33** (2018), no. 6, 443–458.

[17] H. Shariatmadar and G. Behnam Rad, *Evaluation of active controlled structures using subset simulation method*, Nationalpark-Forschung Schweiz **102** (2013), no. 3, 136–157.

[18] J.D. Sørensen, *Notes in structural reliability theory and risk analysis*, Aalborg University, 2004.

[19] P.D. Spanos and I.A. Kougioumtzoglou, *Survival probability determination of nonlinear oscillators subject to evolutionary stochastic excitation*, Appl. Mech. **81** (2014), no. 5, 05101–05116.